Phase Separation and Coalescence, Annihilation of Liquid Crystal Textures during Polymerization of Main-Chain Liquid Crystalline Polyesters

Si-Xue Cheng[†] and Tai-Shung Chung*[,†,‡]

Department of Chemical and Environmental Engineering, National University of Singapore, 10 Kent Ridge Crescent, Singapore 119260, and Institute of Materials Research and Engineering, 10 Kent Ridge Crescent, Singapore 119260

Received: November 6, 1998; In Final Form: February 17, 1999

Using a novel thin film polymerization technique, we have observed the phase separation, coalescence, and annihilation of liquid crystal textures during polymerization of wholly aromatic main-chain liquid crystalline polymer poly(*p*-oxybenzoate/2,6-oxynaphthoate) (P(OBA/ONA)). The polycondensation reaction was conducted and observed in situ on the heating stage of a polarizing microscope. After the melting of monomers, the reaction system started from a homogeneous phase and then changed into a heterogeneous one. The following morphological changes during the entire reaction were observed: generation of anisotropic phase, coalescence of liquid crystal domains, formation of schlieren texture, annihilation of disclinations, and formation of stripe texture. We found all the liquid crystal domains formed in the isotropic melt during the early stage of our polymerization reactions had the disclination strength of +1. The number of defects decreased with increasing reaction time through coalescence and annihilation. At the early stage of polymerization, the dominant factor affecting annihilation rate was the viscosity characteristics at elevated temperatures.

1. Introduction

Main-chain liquid crystalline polymers (MCLCPs) form a class of materials possessing exceptional balance of properties such as high mechanical properties, easy flow, excellent dimensional stability, and chemical resistance. As a result, they have wide applications and received a great deal of attention from both academia and industry. Many review articles and books have described the scientific progress on this subject.[1−6]

Most MCLCPs are polymerized through condensation reactions.[1−6] During the polymerization, liquid crystal (LC) phase separates from isotropic melting when degree of polymerization reaches a certain value, and the melt rapidly becomes turbid since the orientation fluctuations of the growing mesogenic domains are in the range of the wavelength of visible light. Further removal of volatile from the melt is the key to increase the molecular weight. The as-synthesized LC texture and morphology not only determine processability for subsequent process, but also affect the properties of final products.[3] Since melt polymerization starts from a homogeneous phase to a heterogeneous LC phase, different optical textures associated with stringlike and pointlike defects can be observed. Some defects remain in the LCPs solidified from the melt polymerization and the others disappear through annihilation during the reaction. The density and types of defects will strongly affect the rheological behavior, mechanical properties and optical properties of polymeric materials. So the quality of LCPs for end uses is strongly affected by polycondensation conditions, and reproducing a new LCP variant with the same inherent properties still remains a big challenge for industrial producers. However, rare attention has been given by academia to investigate the LC texture formation and evolution during polymerization. Such studies are very limited and most of them focus only on low molecular weight liquid crystals or the systems in which polymer molecular weight does not change.[7−10]

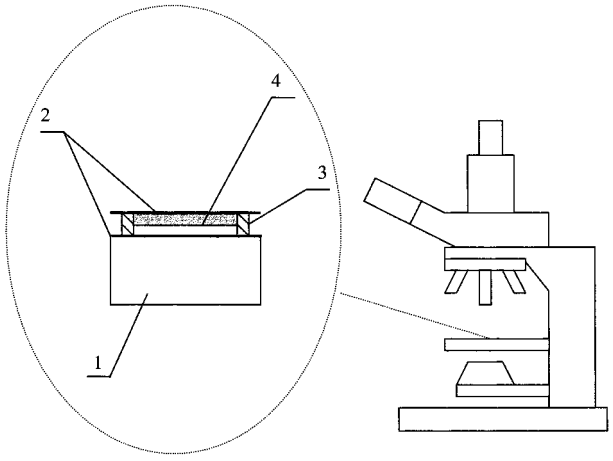

1. Heating stage, 2. Glass slides, 3. Steel ring, 4. Reaction system.

Figure 1. The sample for thin film polymerization.

Geil and co-workers are pioneers to employ thin film polymerization technique to investigate the inherent microstructure of LCPs during the syntheses of a series of aromatic polymers including poly(*p*-oxybenzoate)[11,12] (POBA), poly(2,6-oxynaphthoate)[13] (PONA), poly(meta-oxybenzoate/2,6-oxynaphthoate)[14] (P(mOBA/ONA)), and poly(*p*-oxybenzoate/2,6-oxynaphthoate)[15] (P(OBA/ONA)). The morphology and crystal structure of the polymers were studied by optical and transmission electron microscopes and electron diffraction. Polymers with different inherent crystal structures were obtained after thin film polymerization.

* To whom correspondence should be addressed. E-mail: chencts@nus.edu.sg.
[†] Department of Chemical and Environmental Engineering.
[‡] Institute of Materials Research and Engineering.

10.1021/jp984332q CCC: $18.00
Published on Web 05/12/1999

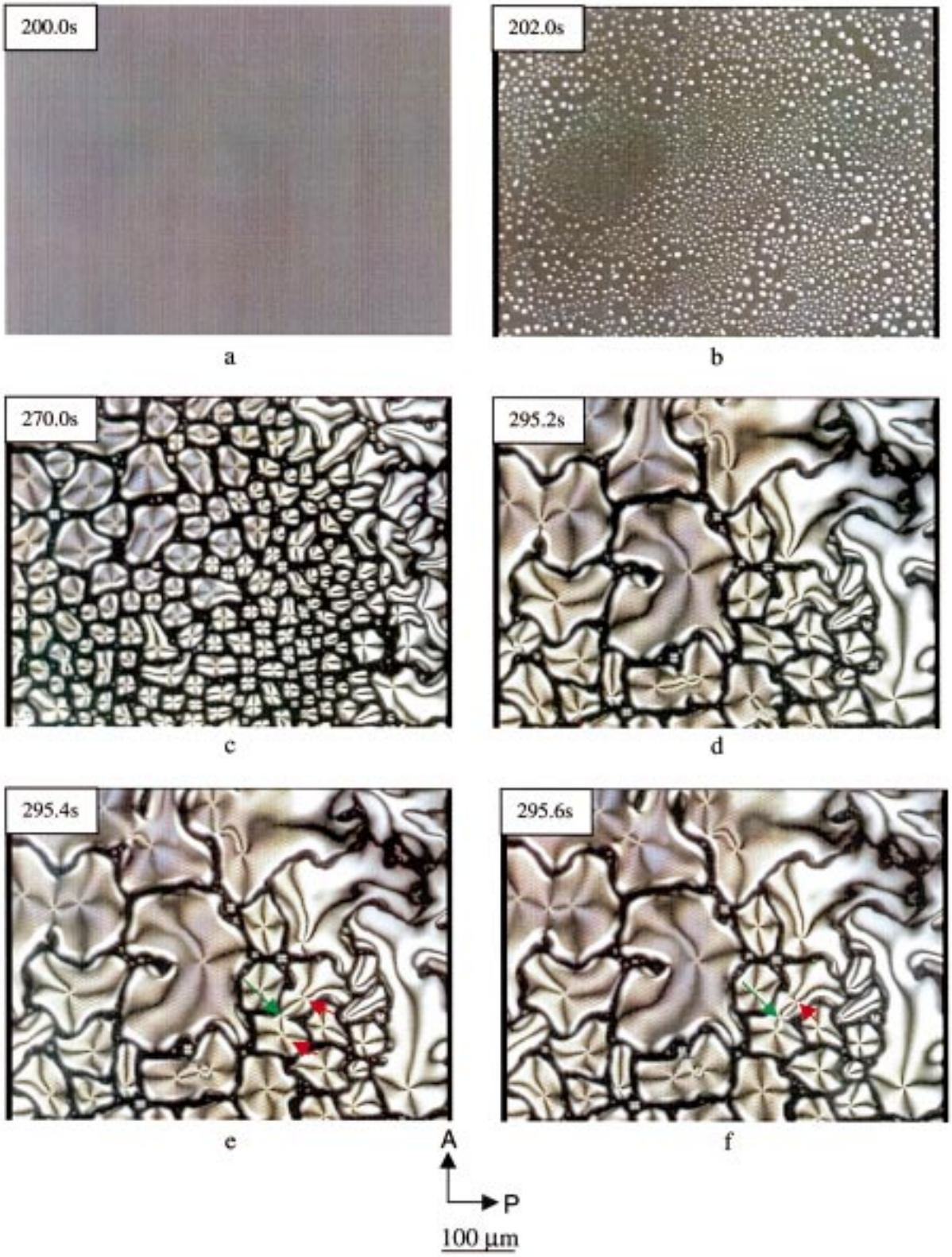

(Figure 2 a−f)

For the LC texture evolution during reaction systems, Yee[16] and Ober[17] have studied the LC texture evolution during curing of liquid crystalline epoxy. They found different curing agent leaded to various LC textures.

Using a novel thin film polymerization technique, we examined and analyzed in situ polycondensation reactions and liquid crystal phase evolution for wholly aromatic LCPs, such as P(OBA/ONA) copolymers and POBA and PONA homopoly-

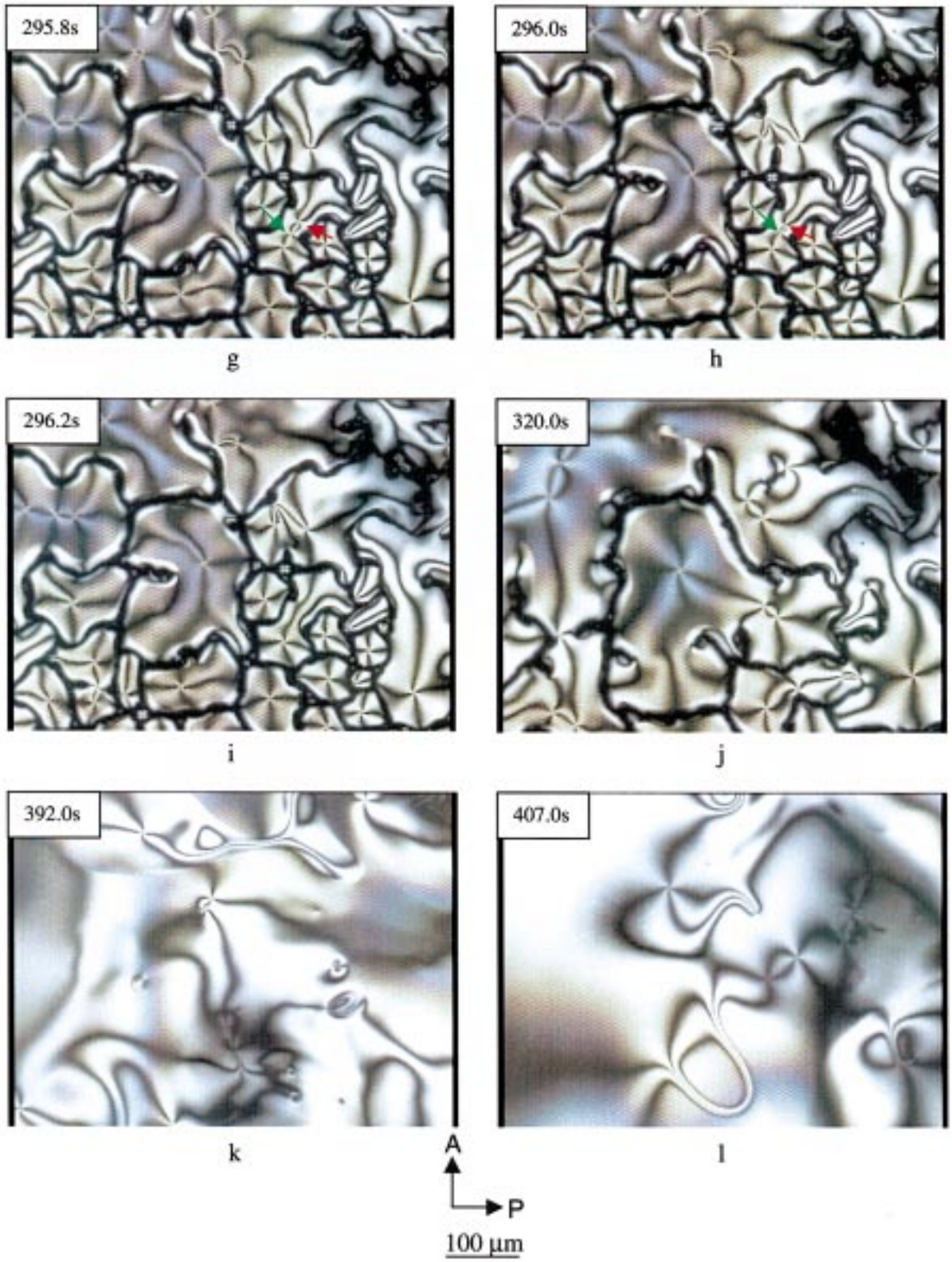

Figure 2. Micrographs showing morphological changes of polymerization reaction system. All the micrographs were obtained from the same area of the same sample. Monomer composition of reaction system was 73/27 ABA/ANA. Reaction temperature was 250 °C.

mers.[18] In our experiments, a thin layer of monomers was sandwiched between two glass slides with a ring spacer and reactions were carried out on a heating stage of a polarizing microscope. Through in situ observation of the microscope, we can use this novel thin film polymerization technique to in situ investigate morphological changes during the reaction and, thus,

unfold the evolution of LC structure in polycondensation reactors. In this paper, we intend to extend our previous work to investigate the whole process of LC texture generation, evolution, and annihilation of different kinds of defects during the polymerization reaction, thereby providing important information for LCP synthesis.

2. Experimental Section

2.1. Preparation of Monomers: *p*-Acetoxybenzoic Acid (ABA) and 2,6-Acetoxynaphthoic Acid (ANA). The monomers were made by the acetylation of p-hydroxybenzoic acid (HBA) and 2,6-hydroxynaphthoic acid (HNA) separately, with acetic anhydride in refluxing toluene in the presence of a catalytic amount of pyridine. The prepared monomer ABA was then purified by recrystallization in butyl acetate. Similarly ANA was purified in methanol. The success of acetylation for both monomers was confirmed by ^{1}H NMR.

2.2. Thin Film Polymerization. Two monomers, ABA and ANA, with certain mole ratios were codissolved in acetone to form a miscible solution. After solvent evaporating, a 0.5 mg monomer mixture was placed on a glass slide. A drop of acetone was deposited on the glass slide to dissolve monomers again. After evaporation of the solvent, a thin layer of reactant mixture was formed and attached to the glass slide and then sandwiched between two glass slides with a ring spacer. The monomers were attached on the bottom slide. The ring spacer was made of stainless steel with a thickness of 0.5 mm. The whole package was placed on a heating stage (Linkam THMS-600) of a microscope and heated to a proposed temperature with a heating rate of 90 °C/min. The sample was held at that specific temperature during the whole reaction process. When heating stage reached the proposed temperature, the reaction time began to be recorded. During the heating, monomers sublimated to the top slide from the bottom one because of the temperature difference between these two slides. After reaching proposed reaction temperature, all monomers were attached on the top slide except the loss, which was less than 5%. Nothing was remained on the bottom slide. The temperature of the top slide was calibrated by testing the melting points of the pure monomers as well as by measuring with thermocouple. The temperature difference between the heating stage set by the programmer and the top slide was 20 ± 2 °C in our experimental temperature range. The polymerization reaction was carried out on the top slide and all the temperatures mentioned refer to the temperatures of the top slide. The reaction process was observed in situ by a polarizing light microscope (Olympus BX50) with crossed polarizers between which a red plate having the retardation of 530 nm was inserted or not inserted. The optical images were recorded by a digital video cassette recorder (DHR-1000NP). The data of the micrographs were analyzed by imaging software (Image-Pro Plus 3.0). The sample for thin film polymerization is shown in Figure 1.

2.3. Characterization. *FTIR Characterization.* The monomers and polymers were characterized by FTIR (Perkin-Elmer FTIR Spectrometer Spectrum 2000.). Polymer sample (in KBr pellet) was prepared by scraping materials from the slide.

3. Results and Discussion

3.1. Phase Separation and Time Evolution of Liquid Crystal Texture during Polymerization Reaction. Using the reaction system with the monomer composition of 73/27 (mole ratio) ABA/ANA at a reaction temperature of 250 °C as an example, we investigated the polycondensation reaction system. During whole polymerization reaction, the system starts from mixed crystals, and melts to homogeneous phase, and then changes into a heterogeneous system with the following sequence of morphological changes: generation of anisotropic phase, coalescence of LC domains, formation of schlieren texture, annihilation of disclinations, and formation of stripe texture.

3.1.1. Generation of Anisotropic Phase: LC Domains. Figure 2 illustrates a set of micrographs showing the typical LC phase separation from a homogeneous phase and time evolution of LC texture in the early stage of thin film polymerization. During the heating, the monomers melted and the whole view area became isotropic melt phase as shown in Figure 2a. In the early stage of polycondensation reaction, oligomers formed in the molten monomer phase. Their molecular weight and chain length increased with reaction time. When the chain length of the oligomers reached a certain value, they formed anisotropic phase (LC phase) and separated from the isotropic melt. Figure 2b shows the reaction induced phase separation process during the polymerization. The dark area in the micrograph is the isotropic phase, while the bright area represents the anisotropic phase. The first sign of forming anisotropic phase was that many bright LC domains instantaneously appeared in the view range. Because of the polydispersity of the chain length, oligomers were partitioned within the isotropic and anisotropic phase according to the chain length.[19] A fraction of relatively longer chain length formed anisotropic domains, while others remained in the isotropic phase.

3.1.2. Coalescence of LC Domains: Formation of Schlieren Texture. After the appearance of anisotropic phase, the size of LC domains quickly increased, and correspondingly the number of domains decreased because of domain growth and coalescence of adjacent LC domains.

Figures 2d−i illustrate a detailed coalescence process. According to previous study,[6] we know that black brushes originating from the points are regions where the director is either parallel or perpendicular to the plane of polarization of incident light, therefore the incident light is extinguished by the crossed polarizers. When rotating the crossed polarizers, the position of the points remains unchanged but the brushes rotate continuously showing that the orientation of the director changes continuously about the disclinations. If the sense of rotation is the same as that of polarizers, the disclination is a positive one. On the contrary, if the sense of rotation is opposite to that of polarizers, the disclination is a negative one. The strength S of a disclination is determined by the number N of the dark brushes around the single disclination: $|S| = N/4$. We found in our experiment all LC domains formed in the isotropic melt had the disclination strength of $+1$. In Figure 2e, the two domains with strength $S = +1$ are indicated by red arrows. When coalescence happened, a negative disclination of strength $S = -1$ as indicated by green arrow formed at the contact point of these two domains as soon as they contacted each other. The process followed was the annihilation of the two defects with opposite signs as shown in Figures 2e−i. After the formation of the disclination of $S = -1$ during coalescence, this disclination (indicated by green arrow) and one of adjacent disclinations of $S = +1$ (indicated by red arrow) immediately moved toward each other and then disappeared together. Figure 3 shows the dependence of distance D between the two disclinations on reaction time t (for the case of Figure 2e−i). The distance decreased with reaction time almost linearly and two disclinations disappeared together after 0.8 s of the coalescence. Thus, a large domain with only one declination of $S = +1$ was formed.[14]

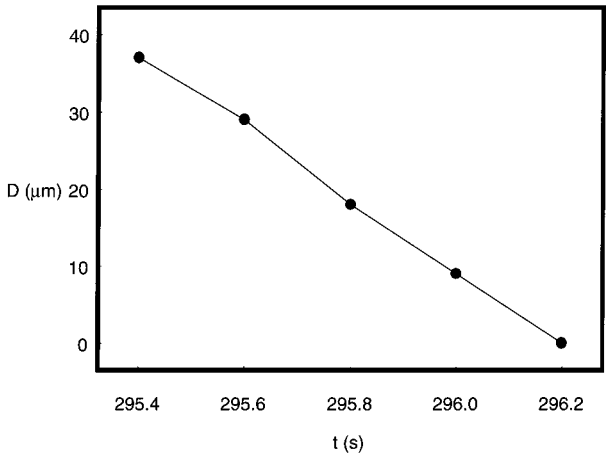

Figure 3. Time dependence of annihilation process after coalescence. Monomer composition of reaction system was 73/27 ABA/ANA. Reaction temperature was 250 °C. (For the case of Figure 2e−i).

The growth of the LC phase occurred when reaction time was in the range from 202 s to 392 s for this sample. As a result, the total view area became anisotropic LC phase and the sum of the strength of all disclinations in the sample tended to be zero. The typical schlieren texture was formed at this moment.

3.1.3. Time Evolution of Schlieren Texture: Annihilation of Disclinations. As we know, the dynamical properties of LCP are quite different from that of LC, but the static properties of LCP are similar to that of LC.[6] In the continuum theory of LC, the distortion energy density is given by:

$$F_d = {}^1/_2 K_1 (\mathrm{div}\mathbf{n})^2 + {}^1/_2 K_2(\mathbf{n} \cdot \mathrm{curl}\mathbf{n})^2 + {}^1/_2 K_3(\mathbf{n} \times \mathrm{curl}\mathbf{n})^2$$

where **n** is the variable director, K_1, K_2, and K_3 are elastic constants for splay, twist, and bend, respectively.[20] According to this formula, the larger the elastic constants are, the higher the distortion energy is. Normally, the elastic constants decrease with increasing temperature, and increase with increasing length of molecules. According to Odijk's deduction, the splay, twist, and bend elastic constants for the polymer chains which are not completely rigid can be expressed as follows:[4]

$K_1 \approx 3K_2$

(if the chain length L is less than the persistence length q)

$K_1 \propto L$

(if the chain length L exceeds the persistence length q)

$$K_2 \approx \phi^{1/3}(q/d)^{1/3}(kT/d)$$

$$K_3 \approx \phi(q/d)(kT/d)$$

where the term (kT/d) redimensionalizes the constant to give the units of force, $\phi = 1$ for thermotropic polymers, and q/d is the persistence ratio. Thus the elastic constants increase with increasing persistence length. If the molecular length exceeds the persistence length, the values of K_2 and K_3 will tend to be constant, while K_1 will increase monotonically with L.

Since the defects are caused by the deformation of molecular chains, they involve very high distortion energy in the case of rigid or semirigid polymers.[7−10,20] Disclinations with opposite signs are trendy to attract each other in order to release the energy. This interaction leads to the annihilation and the decrease in the number of defects. In our polymerization systems, the annihilation between two opposite sign disclinations and annihilation of the loops were two methods to release the excess deformation energy.

A. Annihilation between Two Opposite Disclinations. During the thin film polymerization reaction, we observed that schlieren texture evolved to inversion walls and, at the same time, annihilation occurred between disclinations. The micrographs in Figure 4 were taken from the same area of same sample when the range of reaction time was 441.0−449.4 s. They show the annihilation process of a pair of disclinations with opposite strength $S = +1$ and -1. According to Figure 4, we can see the distance between the pair of disclinations gradually decreased. At last, two disclinations disappeared together. During this process, the molecules within the area rearranged their orientation and yielded a locally perfect orientation after the annihilation.

Figure 5 shows the distance between the two disclinations decreases in an approximately linear manner with the reaction time because the slope of the straight line in logarithmic scale is 1. (Here t_o is the time that two disclinations joined and disappeared.) For the nonreacting systems, the annihilation kinetics follows a power law.[7−10] Our experiment data indicates the annihilation kinetics for reacting system also follows the power law. Although the viscosity increases with the progress of polymerization reaction because of the increase in molecular weight, we have not observed its effect on annihilation. This is due to the fact that the change in viscosity was not obvious because the annihilation happened within a relatively short time interval.

At the beginning of polycondensation reaction, the annihilation occurred very quickly, indicating the molecular weight at this stage was relatively low and thus viscosity of the system was not very high. With an increase in the reaction time, the annihilation rate slowed because the increasing viscosity restricted the motion of disclinations for further annihilation. When the energy needed for the reorganization of molecular orientation was higher than that released by the annihilation of defects, the annihilation process was completely retarded. The annihilation between two pairs of defects during different reaction time intervals in the same sample is compared in Figure 6. In this Figure, the annihilation rate ($v = \mathrm{d}D/\mathrm{d}t$) for the same pair of defects remained approximately the same during the whole annihilation process. For the annihilation occurred during the time interval of 441.0−449.4 s, as already shown in Figure 5, the annihilation rate was about 25 μm/s. While for another annihilation occurred during the time interval of 530−716 s, the annihilation rate was much slower, about 2 μm/s. In our reaction system at 250 °C, no further movement of defects could be observed after reaction time reached 1000 s.

However, annihilation between the defects was a complicated process and not fully understood yet. We found that the annihilation process was affected by many factors. For example, other defects surrounding the particular pair of defects more or less affect the annihilation. In a polymerization system, a more complicated factor is added to the annihilation process due to the elastic constant change because of the increase in molecular weight. However, the annihilation rates for different pairs of disclinations decrease with reaction time is a universal trend.

B. Shrinkage of Loop. Figure 7 shows the typical annihilation of loops for the polymerization at 250 °C. The images were taken at reaction time ranging from 480−546 s. With an increase in the reaction time, the loop gradually shrank, at the same time changed its shape into circular one, and finally disappeared. Time dependence of the loop (indicated by the arrow) area A and perimeter P is shown in Figure 8. (t_o is the time that the

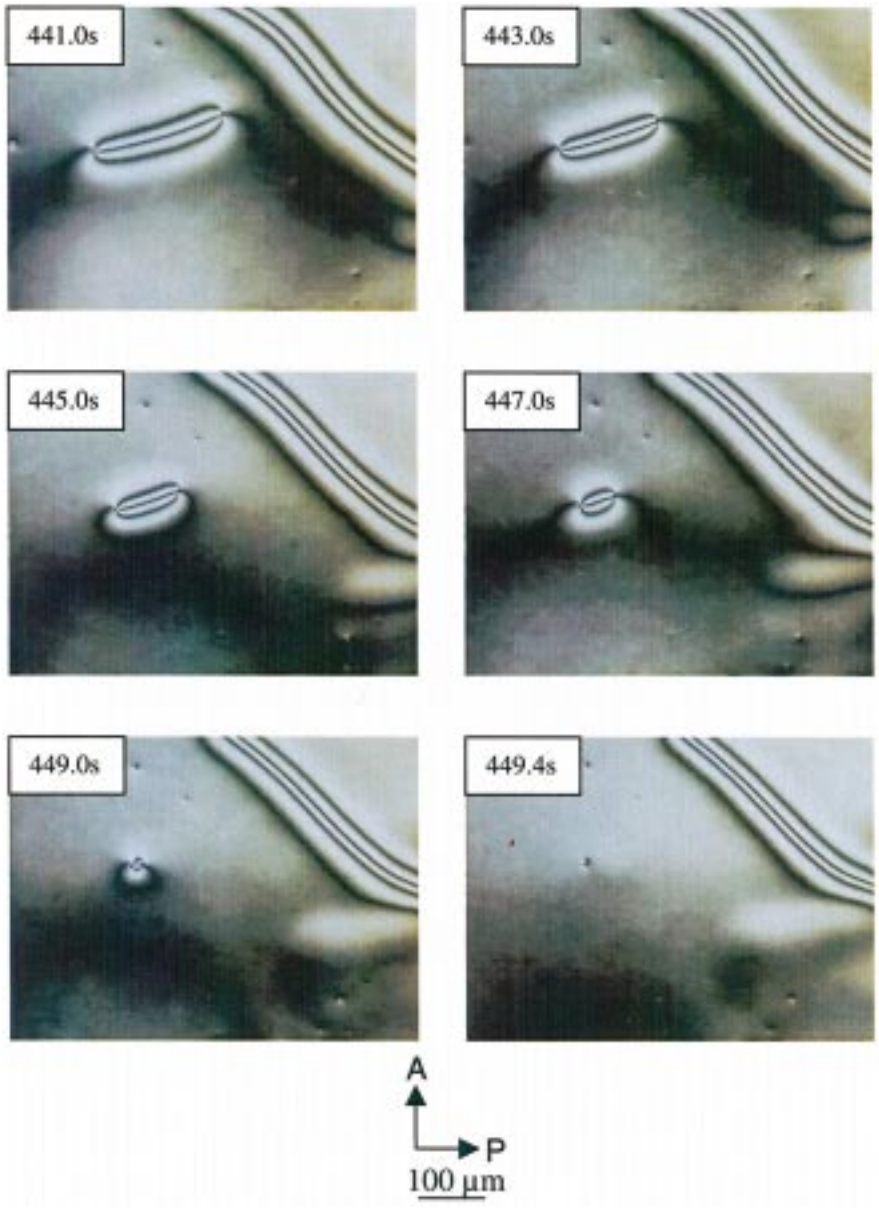

Figure 4. Micrographs showing the annihilation process of a pair of disclinations with opposite signs. All the micrographs were obtained from the same area of the same sample. Monomer composition of reaction system was 73/27 ABA/ANA. Reaction temperature was 250 °C.

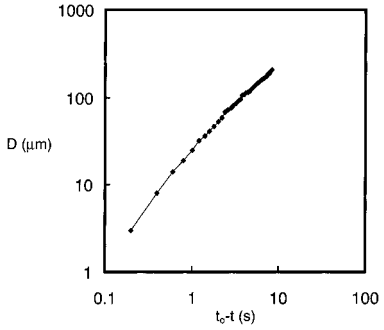

Figure 5. Time dependence of the distance D between a pair of disclinations. The disclinations are shown in Figure 4. t is reaction time, and t_o is the time that two disclinations joined and disappeared. Monomer composition of reaction system was 73/27 ABA/ANA. Reaction temperature was 250 °C.

loop disappeared.) We can find that the decrease in area and perimeter of the loop follows a power law within the middle stage of the shrinkage.

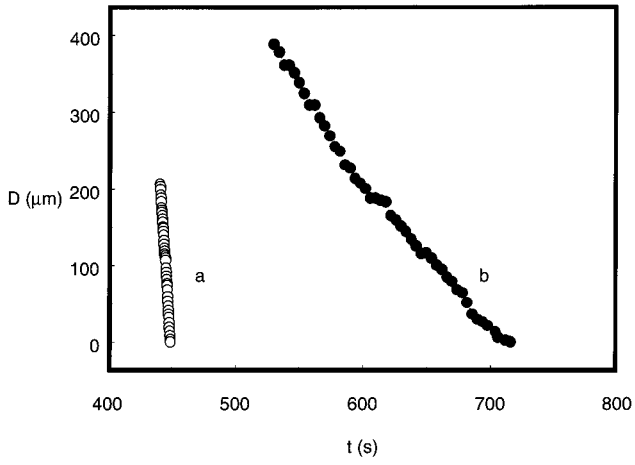

Figure 6. Annihilation of two pairs of disclinations during different reaction time intervals. (a) 441.0−449.4 s and (b) 530−716 s. Monomer composition of reaction system was 73/27 ABA/ANA. Reaction temperature was 250 °C.

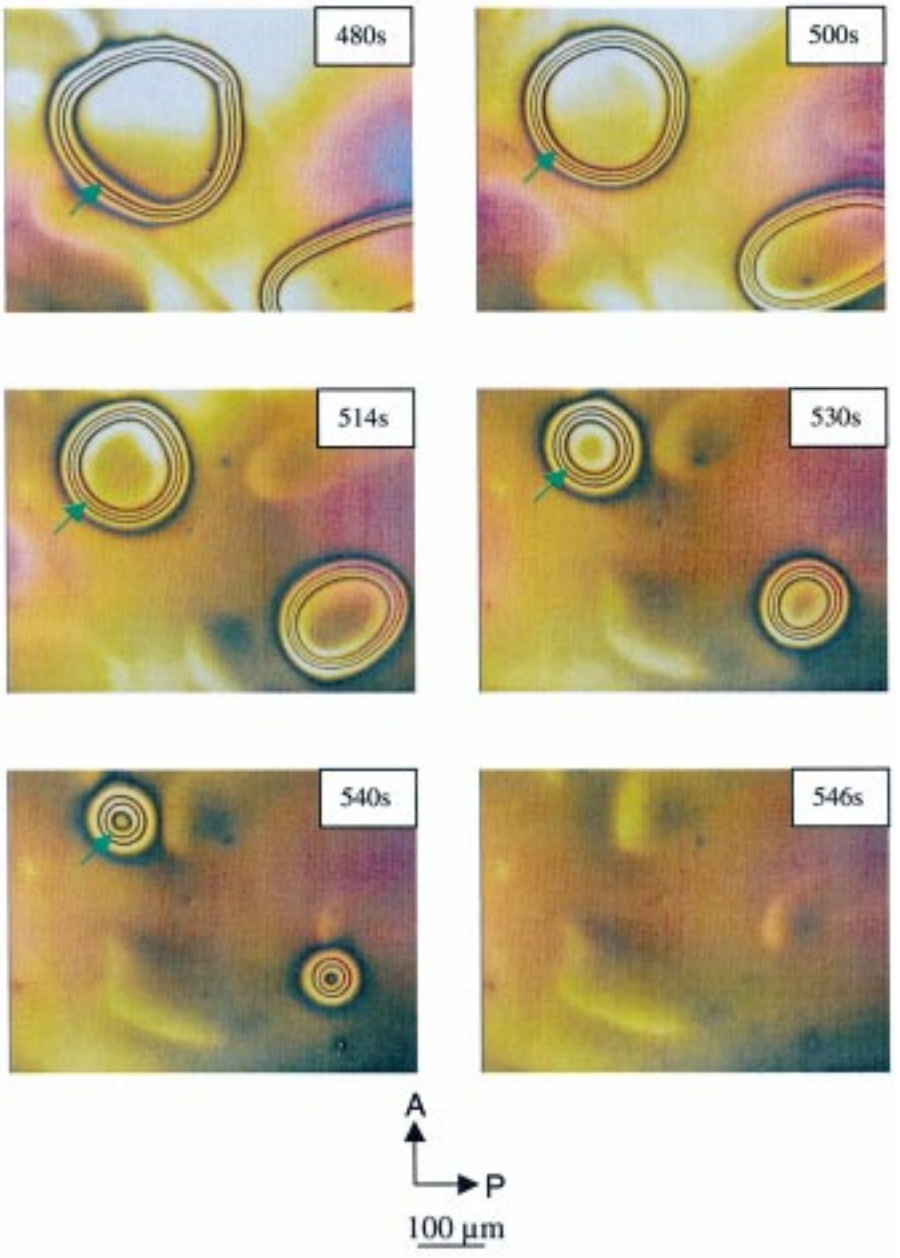

Figure 7. Micrographs showing the shrinkage process of loops. All the micrographs were obtained from the same area of the same sample. Monomer composition of reaction system was 73/27 ABA/ANA. Reaction temperature was 250 °C.

In the reaction systems we investigated, for the pairs of disclinations with opposite signs, in some cases they annihilated and then completely disappeared, while in other cases the distance between two opposite disclinations decreased but defects still existed in the system. For the loops, in some cases they shrank, were annihilated, and then disappeared, while in other cases, they shrank into a small area or a spot and stayed in the system. At the beginning stage of schlieren texture, the density of defects in the reaction system was considerably high. After annihilation, the density dramatically decreased.

3.1.4. Formation of Stripe Texture. LCPs exhibit a variety of textures of different length scales originated from flow and deformation. A frequently observed texture called "stripe texture" or "banded texture" often emerges in the samples in which relaxation or shrinkage of molecular chains occurs. The conditions inducing this texture include: subjecting to shear and/or elongation flow,[21] evaporating the solvent from a lyotropic LC,[22] and quenching a thermotropic LC from high

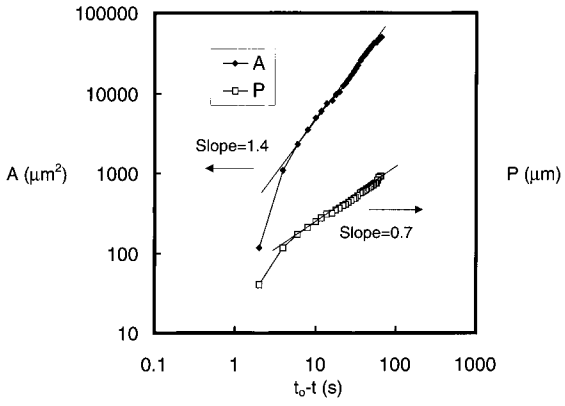

Figure 8. Time dependence of area *A* and perimeter *P* of the loop. The loop is shown in Figure 7. *t* is reaction time, and t_o is the time that the loop disappeared. Monomer composition of reaction system was 73/27 ABA/ANA. Reaction temperature was 250 °C.

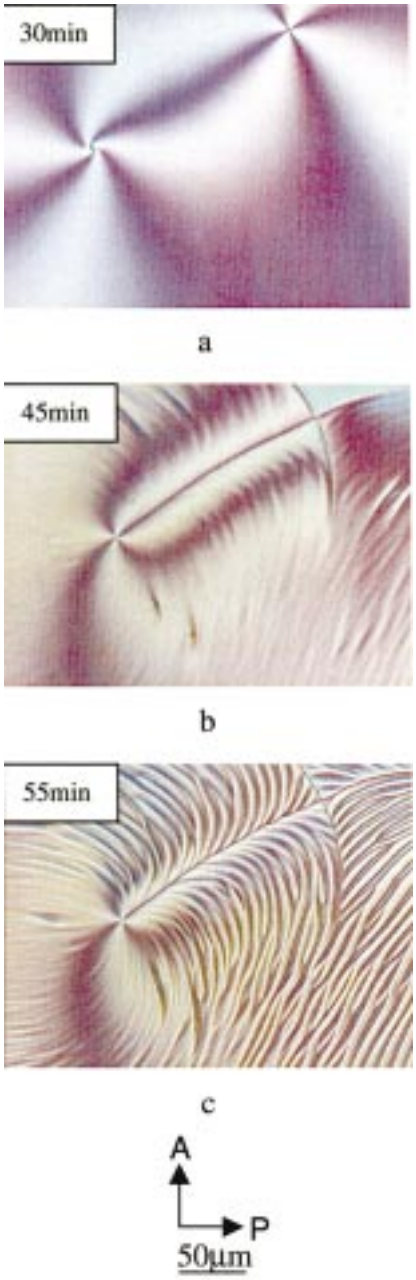

Figure 9. Micrographs showing the formation of stripe structure. All the micrographs were obtained from the same area of the same sample. Monomer composition of reaction system was 73/27 ABA/ANA. Reaction temperature was 250 °C.

temperature.[23] As a consequence of stress relaxation after shear or volume deficiency induced by solvent evaporating or quenching, stripe texture appears while local order does not decrease significantly.[21−23]

In our reaction system, with the increase of molecular weight, the volume deficiency caused the appearance of stripe texture since adhesion to the substrate prevented uniform shrinkage in three dimensions. Figure 9 shows formation of stripe texture at the reaction time ranging from 30−55 min. Figure 9a is the typical schlieren texture with two disclinations of opposite signs. The dark line connecting the defects is quite diffuse, indicating the defects are isolated. After the stripe texture appeared (Figure 9b), the situation changed, the defects are connected by an inversion wall (the sharp dark line). From the stripes in Figure 9c we can deduce that the strength of the left disclination is

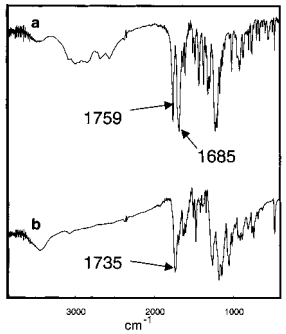

Figure 10. The FTIR spectra of (a) monomers and (b) polymers. Monomer composition was 73/27 ABA/ANA. Reaction temperature was 250 °C.

+1 and the right one is −1 because the macromolecular chain orientation is perpendicular to the stripes. The stripe texture developed fully within more than 10 min. The width of the stripes is about 5 μm.

However, the stripe texture may not appear in some other composition and reaction temperatures if the crystallization occurs first and interrupts the formation of stripe texture.[18]

3.2. FTIR Characterization. During thin film polymerization, ester exchange reactions between acetoxy groups and carboxyl groups occur with elimination of acetic acid.

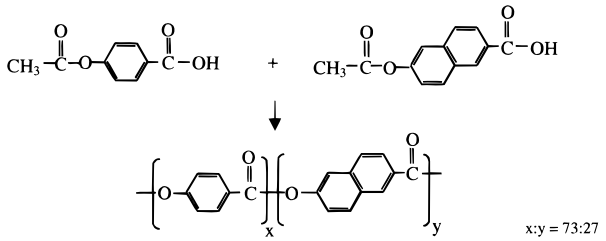

This polycondensation reaction follows second-order kinetics.[24] The detail kinetics study will be reported in our following paper.

Figure 10 shows the FTIR spectra of monomers and thin film polymerization product. Figure 10a is the spectrum of a 73/27 ABA/ANA monomer mixture. The band at 1685 cm^{-1} is $\nu_{C=O}$ of the −COOH group and the band at 1759 cm^{-1} is $\nu_{C=O}$ of the CH_3COO- group. After a 2 h reaction, as shown in Figure 10b, the bands at 1685 and 1759 cm^{-1} almost completely disappear which indicates that nearly all of acetoxy and carboxyl groups are consumed, with a substantial number of ester groups formed in 1735 cm^{-1}. On the basis of these spectra, we believe copolymers are obtained.

3.3. Effect of Reaction Temperature on Annihilation during the Polymerization. To investigate the effect of the reaction temperature on annihilation, we conducted thin film polymerizations at different reaction temperatures from 230 to 310 °C for 73/27 ABA/ANA system. The annihilation processes at different areas of the same sample as well as different samples with same reaction conditions were recorded and the annihilation rates v were calculated. The results are summarized in Figure 11, where t_1 is the time for the appearance of the anisotropic phase. The dashed line represents that annihilation occurred before formation of schlieren texture (before total view area became LC phase), while the solid line represents that annihilation occurred after formation of schlieren texture (after total view area became LC phase). The length of the line indicates the range of annihilation rates.

Figure 11 suggests that the annihilation rates for different pairs of disclinations vary in a wide range even during the same

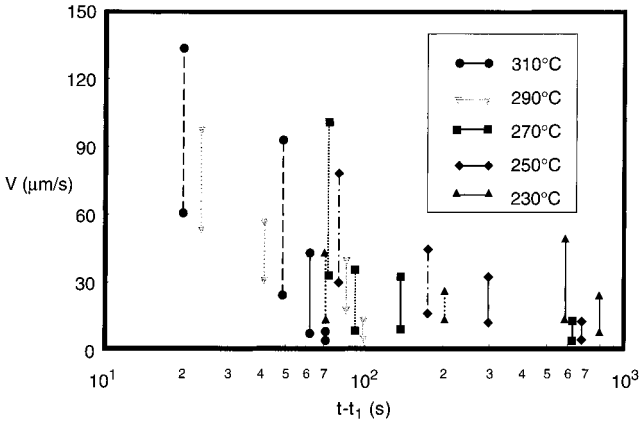

Figure 11. Time dependence of annihilation rate for reaction systems at different temperatures. t is reaction time, and t_1 is the time of appearance of anisotropic phase. (a) 310 °C: $t_1 = 37$ s, (b) 290 °C: $t_1 = 90$ s, (c) 270 °C: $t_1 = 140$ s, (d) 250 °C: $t_1 = 202$ s and (e) 230 °C: $t_1 = 510$ s. Monomer composition of reaction systems was 73/27 ABA/ANA.

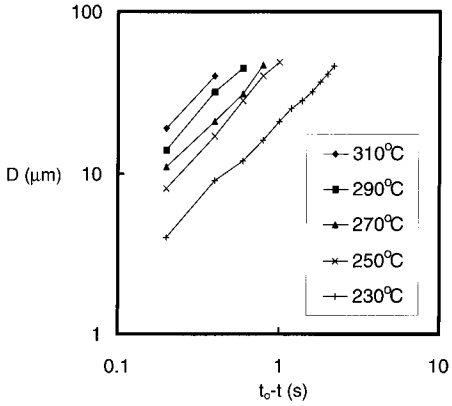

Figure 12. Comparison of typical annihilation processes when the fraction of LC phase is 70% at different reaction temperatures. t is reaction time, and t_o is the time that two disclinations joined and disappeared. Monomer composition of reaction systems was 73/27 ABA/ANA.

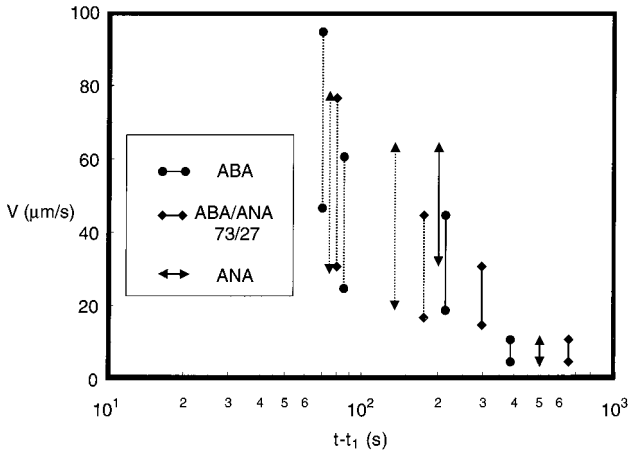

Figure 13. Time dependence of annihilation rate for reaction systems with different monomer composition. t is reaction time, and t_1 is the time of appearance of anisotropic phase. (a) ABA: $t_1 = 246$ s, (b) 73/27 ABA/ANA: $t_1 = 202$ s and (c) ANA: $t_1 = 328$ s. Reaction temperatures were 250 °C.

reaction time interval and at the same reaction temperature. For example, the highest and lowest annihilation rates we have observed were 133 and 60 μm/s, respectively, when the reaction temperature was 310 °C and $t-t_1$ was around 15 s. However, Figure 11 clearly exhibits that, for most cases, annihilation rate decreases with increasing reaction time as we have mentioned before. In addition, the higher the polymerization temperature we used, the faster the change of annihilation rate is. This is due to the fact that viscosity plays a critical role to determine the speed of the annihilation since a higher reaction temperature causes a higher reaction rate and a faster increase in viscosity.

The speed of the annihilation monotonically decreases with the increasing reaction time if polymerization reactions take place at temperatures ranging from 250 to 310 °C. However, the situation changed when the reaction temperature was low: 230 °C. Before the total view area became an anisotropic phase, the annihilation rate was around 15−45 μm/s when $t - t_1 = 51$ s and 15−27 μm/s when $t - t_1 = 160$ s. After the total view area became an anisotropic phase, the annihilation rate increased to 15−50 μm/s when $t - t_1 = 388$ s. It is a challenge to explain the increase in annihilation rate. The possible explanation for this interesting phenomenon is the change in elastic constants played a more important effect than the change in viscosity. Since the reaction at 230 °C was slow, the system viscosity did not change significantly from $t - t_1 = 51$ to 388 s. But the elastic constants increased with an increase in molecular length, thus the distortion energy of the system increased and resulted in a relatively high annihilation rate.

The annihilation after coalescence of LC domains when the fraction of LC phase was 70% (before the total view area became an anisotropic phase) at different reaction temperatures is compared in Figure 12. Figure 12 suggests that annihilation rate increases with the increasing reaction temperature. This phenomenon also shows the reaction rate and viscosity are important factors affecting the annihilation since a higher temperature resulted in lower viscosity.

3.4. Annihilation in Reaction Systems with Different Monomer Composition. We also studied the annihilation process during homopolymerizations of pure ABA and pure ANA at 250 °C. Results are illustrated in Figure 13. The relationship between the annihilation rate and the reaction time for systems with different monomer composition is similar. Both annihilation rate and its range decrease with an increase in $t - t_1$. Although the molecular structures will affect the values of elastic constants, and thus affect the annihilation, we have not observed obvious difference in annihilation rate among these three systems. This indicates that these three systems might have similar values of elastic constants at early stage of polymerization.

4. Conclusions

We have observed phase separation, coalescence, and annihilation of liquid crystal textures during polymerization of liquid crystalline polyesters by a novel thin film polymerization technique. The polycondensation system continuously changed from random monomer melt to highly orientated polymers through the following morphological changes: generation of anisotropic phase, coalescence of LC domains, formation of schlieren texture, annihilation of disclinations, and formation of stripe texture. All the LC domains formed in the isotropic melt during the early stage of polymerization for these wholly aromatic liquid crystalline polyesters had the disclination strength of +1. The number of defects decreased with increasing reaction time through coalescence and annihilation. In most cases, the higher reaction temperature we used, the faster the annihilation rate was. At the early stage of polymerization, the dominant factor affecting annihilation rate was the low viscosity characteristics at elevated temperatures. For reaction systems

with different monomer composition, their annihilation patterns were similar.

Acknowledgment. The authors would like to express their gratitude to National University of Singapore (NUS) for the financial support with Research Fund RP 950696. Thanks are also due to Prof. P. H. Geil at University of Illinois for providing us many useful and knowledgeable comments, Dr. S. Mullick for providing the monomers, and Dr. W. Wang, Mr. S. L. Liu, Ms. W. H. Lin, and Mdm. L. K. Leong for their kind help and useful comments. Special thanks are due to the Institute of Materials Research and Engineering (IMRE) of Singapore for the equipment.

References and Notes

(1) Chung, T. S. *Polym. Eng. Sci.* **1986**, *26*, 901.
(2) Chung, T. S.; Calundann, G. W.; East, A. J. *Encyclopedia of Engineering Materials* **1989**, *2*, 625.
(3) Collyer, A. A. *Liquid Crystal Polymers: From Structures to Applications*; Elsevier Science Ltd.: London, 1992.
(4) Shibaev, V. P.; Lam, L. *Liquid Crystalline and Mesomorphic Polymers*; Springer-Verlag: New York, 1994.
(5) Economy, J. *Mol. Cryst. Liq. Cryst*. **1989**, *169*, 1.
(6) Donald, A. M.; Windle, A. H. *Liquid Crystalline Polymers*; Cambridge University Press: Cambridge, 1992.
(7) Wang, W. *Liq. Cryst.* **1995**, *19*, 251.
(8) Liu, C.; Muthukumar, M. *J. Chem. Phys.* **1997**, *106*, 7822.
(9) Shehadeh, H. M.; Mcclymer, J. P. *Phys. Rev. Lett.* **1997**, *79*, 4206.
(10) Shiwaku, T.; Nakai, A.; Hasegawa, H.; Hashimoto, T. *Polym. Commun.* **1987**, *28*, 174.
(11) Rybnikar, F.; Yuan, B. L.; Geil, P. H. *Polym.* **1994**, *35*, 1863.
(12) Rybnikar, F.; Liu, J.; Geil, P. H. *Macromol. Chem. Phys.* **1994**, *195*, 81.
(13) Liu, J.; Rybnikar, F.; Geil, P. H. *J. Polym. Sci. Phys. B* **1992**, *30*, 1469.
(14) Rybnikar, F.; Yuan, B. L.; Geil, P. H. *Polymer* **1994**, *35*, 1831.
(15) Liu, J.; Rybnikar, F.; Geil, P. H. *J. Macromol. Sci.* **1996**, *35*, 375.
(16) Lin, Q.; Yee, A. F.; Sue, H. J.; Earls, J. D.; Hefner, R. E. *J. Polym. Sci. Phys. B* **1997**, *35*, 2363.
(17) Shiota, A.; Ober, C. K. *Macromolecules* **1997**, *30*, 4278.
(18) Cheng, S. X.; Chung, T. S.; Mullick, S. *Chem. Eng. Sci.* **1999**, *54*, 663.
(19) Nakai, A.; Wang, W.; Hashimoto, T.; Blumstein, A.; Maeda, Y. *Macromolecules* **1994**, *27*, 6963.
(20) de Gennes, P. G.; Prost, J. *The Physics of Liquid Crystal*; Clarendon Press: 1993.
(21) Viney, C.; Putnam, W. S. *Polymer* **1995**, *36*, 1731.
(22) Wang, W.; Lieser, G.; Wegner, G. *Liq. Cryst.* **1993**, *15*, 1.
(23) Chen, S.; Song, W.; Jin, Y.; Qian, R. *Liq. Cryst.* **1993**, *15*, 247.
(24) Williams, P. A.; Han, X.; Padias, A. B.; Hall, H. K. *Macromolecules* **1996**, *29*, 1874.